AGU PUBLICATIONS

JGR

Journal of Geophysical Research: Oceans

RESEARCH ARTICLE

10.1002/2013JC009169

Key Points:
- Vertical velocities in the upper ocean from quasi-geostrophic theory
- Description of mesoscale eddy in the Upwelling Canary Region
- Multiplatform experiment combining in situ and remote sensing observations

Correspondence to:
S. Ruiz,
simon.ruiz@imedea.uib-csic.es

Citation:
Ruiz, S., J. L. Pelegrí, M. Emelianov, A. Pascual, and E. Mason (2014), Geostrophic and ageostrophic circulation of a shallow anticyclonic eddy off Cape Bojador, *J. Geophys. Res. Oceans*, *119*, 1257–1270, doi:10.1002/2013JC009169.

Received 31 MAY 2013
Accepted 27 DEC 2013
Accepted article online 4 JAN 2014
Published online 22 FEB 2014

Geostrophic and ageostrophic circulation of a shallow anticyclonic eddy off Cape Bojador

Simón Ruiz[1], Josep L. Pelegrí[2], Mikhail Emelianov[2], Ananda Pascual[1], and Evan Mason[1]

[1]Instituto Mediterráneo de Estudios Avanzados (CSIC-UIB), Department of Marine Tecnologies, Operational Oceanography and Sustainability, Esporles, Spain, [2]Institut de Ciències del Mar, Department of Physical and Technological Oceanography, CSIC, Passeig Maritim de la Barceloneta, Barcelona, Spain

Abstract A shallow mesoscale anticyclonic eddy, observed south of the Canary Islands with satellite altimetry, has been intensively studied with multiparametric sampling. Hydrographic data from a CTD installed on an undulating Nu-shuttle platform reveal the presence of a mesoscale anticyclonic eddy of ~125 km diameter. The difference in sea level anomaly (SLA) between the interior and the edge of the eddy, as determined from altimetry, is ~15 cm, which compares well with the maximum dynamic height differences as inferred using a very shallow reference level (130 m). Further, the associated surface geostrophic velocities, of about 35 cm s^{-1} in the northeast and southwest edges of the eddy, are in good agreement with direct velocity measurements from the ship. Deep rosette-CTD casts confirm that the structure is a shallow eddy extending no deeper than 250 m before the fusion with another anticyclone. The SLA-tendency (temporal rate of change of sea surface height) indicates a clear northwestward migration during the two first weeks of November 2008. Applying an eddy SSH-based tracker, the eddy's velocity propagation is estimated as 4 km d^{-1}. Use of the QG-Omega equation diagnoses maximum downward/upward velocities of about ± 2 m d^{-1}. The instability of the Canary coastal jet appears to be the mechanism responsible for the generation of the shallow anticyclonic eddy.

1. Introduction

Intensive research on the mesoscale ocean circulation south of the Canary Islands, in the coastal transition zone off Northwest Africa, began in the early 1990s. A number of synoptic cruises revealed different aspects of the dynamics of the mesoscale eddies generated topographically as the Canary Current flows around the Canary Islands [*Arístegui et al*., 1994, 1997; *Barton*, 1998; *Barton et al*., 1998, 2004; *Sangrà et al*., 2005, 2007]. These eddies interact strongly with filaments generated either at the coastal upwelling region, through baroclinic instability processes [*Barton*, 1998; *Barton et al*., 1998, 2004], or downstream of the tallest islands, through wind sheltering [*Barton et al*., 2000]. The ubiquitous presence of these topographic eddies in sea surface temperature (SST) imagery [*Hernández-Guerra et al*., 1993; *Hernández-Guerra and Nykjaer*, 1997; *Barton et al*., 1998; *Pacheco and Hernández-Guerra*, 1999; *Borges et al*., 2004] and their relevance to biogeochemical processes [*Arístegui et al*., 1997; *Basterretxea and Arístegui*, 2000; *García-Muñoz et al*., 2005; *Pelegrí et al*., 2005, 2006; *González-Dávila et al*., 2006; *Piedeleu et al*., 2009; *Brochier et al*., 2011] drew so much attention that little was said about the possibility that some of these eddies had a different origin. The only other proposed generation mechanism was Ekman pumping induced by the horizontal shear in the wind field as it flows past the islands [*Barton et al*., 2000; *Jiménez et al*., 2008; *Piedeleu et al*., 2009].

More recently, *Sangrà et al*. [2009] raised the possibility that some westward propagating eddies, which begin their journey from the lee of the Canary Islands, may have formed through instability processes in the coastal upwelling region. This hypothesis has been explored by *Benítez-Barrios et al*. [2011] by examining the distribution of properties, including vertical velocities, in a single eddy-resolving cruise that stretched from the continental shelf to south of the central and eastern islands. These authors found pairs of eddies of opposite sign (dipoles) with quite different characteristics, in terms of the thermal structure and the intensity of the vertical flow. They ascribed the relatively deep and intense dipoles to topographic origin and suggested the shallower and weaker ones to be produced through instability of the coastal upwelling jet. The analysis, however, was limited by the lack of observations of the time evolution of the property fields.

In relation to the topographically generated eddies, an important open question has been their role in bringing nutrients to the euphotic layers. In particular, based on the surface distribution of chlorophyll, it has been proposed that upwelling and downwelling motions take place near the core of cyclonic and anticyclonic eddies [*Arístegui et al*., 1997; *Barton*, 1998; *Basterretxea and Arístegui*, 2000]. While this is true during the generation process, when the entire upper thermocline rises or sinks as it seeks geostrophic adjustment, this does not need to remain true shortly after the eddy has developed. At these later times we may expect that upwelling and downwelling movements will respond to the eddy's temporal evolution, associated with changes in the density distribution resulting from horizontal variations in the geostrophic current, the so-called convergence or divergence of the Q-vector [*Gomis et al*., 2001].

Benítez-Barrios et al. [2011] carried out what, to our knowledge, is the only quantitative study of the vertical velocity field associated with mesoscale structures south of the Canary Islands. By solving the Q-vector formulation of the Omega equation, they found the region to be characterized by patches of positive and negative vertical velocities, apparently associated with different azimuthal regions of the eddy. The maximum vertical velocities, in the range between -12 and 18 m d^{-1}, were observed around deep topographic eddies, while values typically several times smaller were linked to the shallower eddies located close to the coastal upwelling front. Only a deep anticyclonic eddy, attached south of the island of Fuerteventura, displayed substantial downwelling near its core.

The work presented here aims at providing further insight into the origin and evolution of eddies found south of the Canary Islands. Our objective is to use in situ and remote sensing data to characterize the three-dimensional circulation (geostrophic and ageostrophic) of a shallow mesoscale anticyclonic eddy off Cape Bojador. The eddy was tracked during the cruise, shortly after its formation, with real-time altimetry data but here we make use of the more accurate delayed-mode altimetry data to identify its initial evolution. The eddy was carefully sampled before its fusion with an offshore anticyclonic eddy, and sampled again immediately afterward. Here we look at the three-dimensional distribution of different properties prior to and after the fusion. In particular, we examine the horizontal and vertical velocity fields of the initial eddy. Horizontal velocities are determined through Vessel-Mounted Acoustic Doppler Current Profiler (VM-ADCP) measurements, the trajectory of a subsurface drogged drifter, and both hydrographic and altimetry data. The quasi-geostrophic vertical velocity field is calculated solving the Q-vector form of the Omega equation.

The article is organized as follows. Section 2 describes the multiparametric in situ data set and the methods used in their analysis. Section 3 presents the results obtained through the data analysis, both in terms of vertical velocities and the origin and temporal evolution of the eddy. Section 4 summarizes our findings and discusses those mechanisms that may lead to the generation of shallow eddies; this section ends with several concluding remarks.

2. Data and Methods

The CANOA-08B cruise took place on board the R/V Sarmiento de Gamboa from 2 to 29 November 2008. The campaign involved multiparametric in situ sampling in the region off NW Africa, from Cadiz to Cape Verde and from the shelf break to the deep ocean: the measurements included hydrographic stations with Conductivity-Temperature-Depth (CTD) casts and water samples from a 24 Niskin-bottle rosette; continuous velocity data down to about 600 m depth with the VM-ADCP; CTD sampling with an undulating Nu-Shuttle platform; and the deployment of drifters drogued at about 100 m depth. These measurements were complemented with remote sensing data (SST and altimetry) for the whole NW Africa region. Some results, related to the large-scale distribution of water properties, have been presented by *Pastor et al*. [2012] and *Peña-Izquierdo et al*. [2012]. In this study, we focus on data collected south of the Canary Islands (Figure 1).

2.1. Hydrography and VM-ADCP Data

Between 9 and 11 November 2008, hydrographic observations were gathered south of the Canary Islands using a Nu-Shuttle, an undulating towed vehicle equipped with sensors. The Nu-shuttle survey consisted of four parallel northeast-southwest transects within a box $\sim$35 km wide and $\sim$150 km long (Figure 1). The towed instrument recorded CTD data following a saw-tooth trajectory between 30 and 130 m depth; the ship's velocity during the sampling was about 8 knots. Data processing steps include spike removal, thermal lag correction, and vertical averaging every 5 m. The final horizontal resolution along each transect is $\sim$2 km. Additional details of the Nu-shuttle data processing are available in the technical report prepared by *Emelianov et al*. [2009].

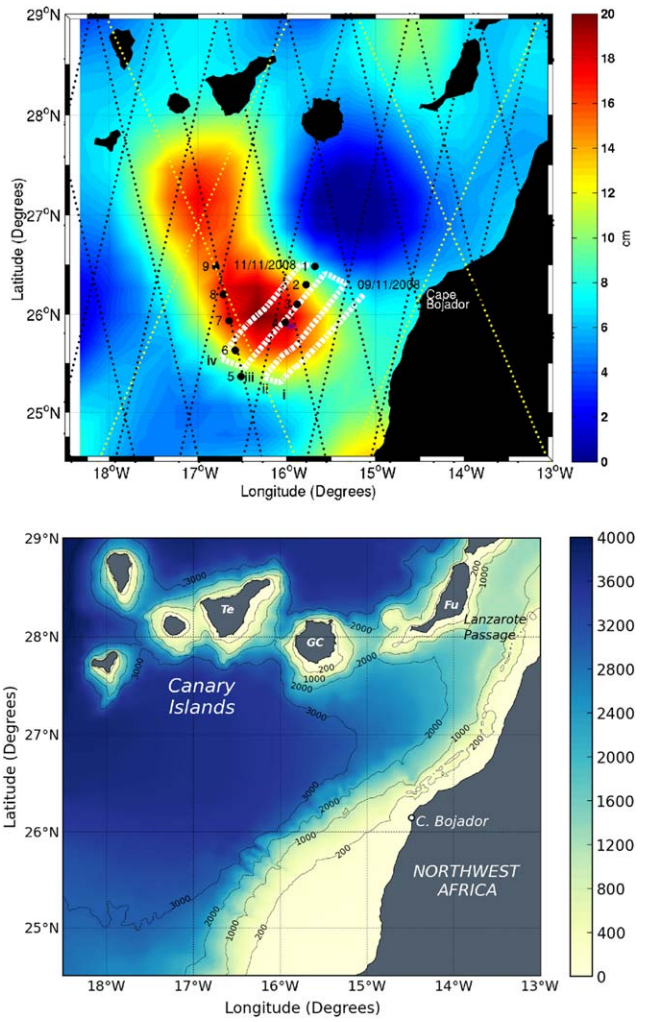

Figure 1. (top) Study area south of the Canary Island (Northeast Atlantic Ocean). White dashed line corresponds to Nu-Shuttle transects ((i)–(iv)), ordered in time and crossing the eddy initially through its edge (transect (i)) and finally near its core (transect (iv)). Black dots correspond to deep CTD-rosette casts performed on 11 November 2008 (stations 1–4), just a few hours after completing the Nu-Shuttle survey, and on 28 November 2008 (stations 5–9), 2 weeks later. Blue asterisk indicates the launch position of a surface drifter buoy. Background color corresponds to altimetry SLA for 10 November 2008. (bottom) Bathymetry of the study area.

On 11 November 2008, just after completing the Nu-shuttle sampling, four CTD casts were performed using a SeaBird 911 Plus probe. The stations were carried out along a North-South radial section, from the periphery toward the center of the eddy (Figure 1, CTDs 1–4), at roughly 30 km spacing and reaching either 500 or 1000 m depth. Two weeks later, on 28 November 2008, the vessel revisited the area, sampling five additional deep stations (CTD casts 5–9, down to 1500 m), at about 40 km intervals. All CTD stations were positioned (Figure 1) so as to cross the eddy, following near real-time altimetry data delivered by AVISO with a 6 day delay. The original vertical resolution of all CTD casts is 1 m but, to be consistent with the Nu-shuttle observations, the CTD data were averaged into 5 m bins. More details on the standard CTD data processing are also available in *Emelianov et al*. [2009].

A 75 kHz VM-ADCP was used to collect velocity data. On 2 November, just after starting the cruise, the instrument was calibrated in shallow waters, using bottom tracking acquisition and following the methodology described by *Griffiths* [1994] and *Ruiz et al*. [2002]. A misalignment angle of 46.22° and scale factor of 1.005 were obtained and considered in the configuration file for the instrument. Final velocity profiles, time averaged every 5 min, have vertical resolution of 8 m [*Emelianov et al*., 2009].

2.2. Surface Drifters

One subsurface drifter was deployed on 12 November 2008 in the center of the area sampled by the Nu-shuttle platform (Figure 1). The drifter consists of a surface buoy and a subsurface drogue at about 100 m depth that minimizes wind drift or other ageostrophic motions in the surface mixed layer. Inside the surface buoy a transmitter (ARGOS system) sends periodic latitude and longitude positioning for the tracking of surface ocean trajectories. Unfortunately, the communication with the drifter was lost after eight days so only a short, but valuable, data series is available for analysis.

2.3. Satellite Altimetry

There is considerable literature on the use and quality of altimeter data for the study of mesoscale variability in the world ocean [*Le Traon et al*., 1998; *Brachet et al*., 2004; *Pascual et al*., 2006]. During the CANOA-08B

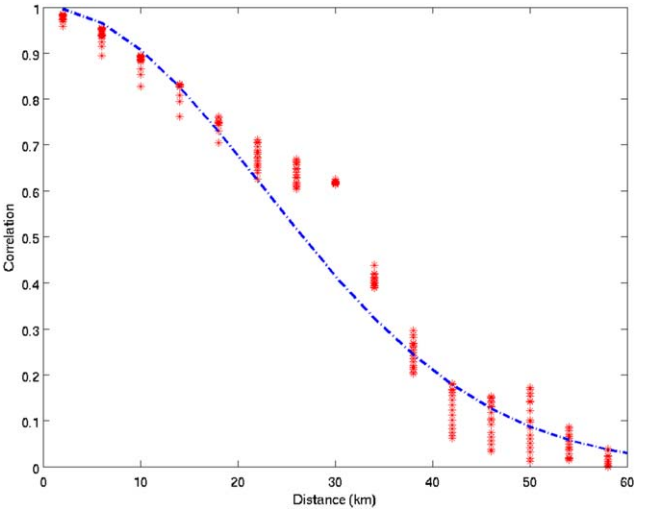

Figure 2. Spatial correlation for dynamic height as derived from hydrographic data at 65 m depth.

cruise, standard daily altimetric maps of Absolute Dynamic Topography (ADT) and Sea Level Anomaly (SLA), as provided by AVISO, were received in near real-time (6 day delay) on board the R/V Sarmiento de Gamboa. For the altimetric analysis described in section 3, the delayed-mode "up-to-date" product has been used. This product is better in quality because it is based on the best sampling available in time through the merging of data from all available satellites [*SSALTO/DUACS User Handbook*, 2013]. The interpolated gridded fields are the outcome of combining data from two different satellites (Jason-1 and Envisat at the time of the CANOA-08B cruise) through an optimal interpolation scheme that uses a 125 km correlation scale at the latitudes of the cruise [*Le Traon et al*., 2003]. The resolution of the interpolated products is 0.25° on a Mercator grid. The mean error of the altimetry maps for the study area is about 10% of the total signal (not shown), which confirms the reliability of this product for the discussion of the characterization and temporal evolution of the eddy. The ADT field is obtained by adding a Mean Dynamic Topography (MDT) to the SLA [*Rio and Hernandez*, 2004]. Finally, from the horizontal gradients of the ADT fields, it is possible to estimate geostrophic velocities, see *Pascual et al*. [2009] for further details.

2.4. Optimal Statistical Interpolation

The hydrographic data set and VM-ADCP measurements are interpolated onto a regular grid through an Optimal Statistical Interpolation (OSI) scheme that has been widely and successfully applied to oceanography, including the estimation of observed and derived variables [*Gomis et al*., 2001; *Allen et al*., 2001]. The scheme analyzes observation increments, i.e., the difference between the observations and the background field. The background, or first guess, field is estimated using a local polynomial fit to the observations [*Thiébaux and Pedder*, 1987].

A simple Gaussian function for the correlation model between observations is set up with a correlation length scale of 30 km, inferred from actual data (Figure 2). The aliasing problem may be significant when mesoscale phenomena are studied with a limited number of observations in time and space. To avoid this problem, an additional low-pass filter with a cut-off length scale of 40 km is applied to select those scales well resolved by the sampling. For an exhaustive description and performance of the scheme, including the sensitivity of the estimated field to the analysis parameters, see *Gomis et al*. [2001].

2.5. Quasi-Geostrophic Vertical Velocity

Since vertical velocities cannot yet be directly measured in the oceans with sufficient accuracy, indirect methods have been developed to estimate this variable. A common approach to determine the vertical velocity, *w*, is based on the quasi-geostrophic (QG) Omega equation, here presented in the vector Q formulation [*Hoskins et al*., 1978]:

$$f^2\frac{\partial^2 w}{\partial z^2}+\left(\frac{\partial^2}{\partial x^2}+\frac{\partial^2}{\partial y^2}\right)\left(N^2 w\right)=\nabla_h\cdot\mathbf{Q} \tag{1}$$

where

$$\mathbf{Q}=\left[2f\left(\frac{\partial v}{\partial x}\frac{\partial u}{\partial z}+\frac{\partial v}{\partial y}\frac{\partial v}{\partial z}\right),-2f\left(\frac{\partial u}{\partial x}\frac{\partial u}{\partial z}+\frac{\partial u}{\partial y}\frac{\partial v}{\partial z}\right)\right]$$

and (u,v) are the horizontal geostrophic velocity components in the west-east and south-north directions (x,y), and z is the (positive upward) vertical coordinate; f is the Coriolis parameter and N is the buoyancy frequency. In this particular study, the upper and lower boundaries have been set as $w = 0$, while Neumann conditions are used at the lateral boundaries. For a detailed study on the use of the Omega equation to diagnose vertical motions in the ocean, see *Pinot et al*. [1996].

3. Results

3.1. Surface Variability From Altimetry

Interpolated altimetry data from the beginning of October (1 month before in situ sampling) to the end of November 2008 (after in situ sampling) complement the hydrographic records and provide a description of the temporal evolution of the surface circulation. The images from 1 and 8 October 2008 show three large mesoscale features in the area south of the Canary Islands: an elongated structure formed by two anticyclones and a weaker cyclone to the east. In this study, we focus on the anticyclonic eddy (hereinafter AE-Mioko) sampled near the African coast (Figure 3a). On 15 October, the ~125 km diameter AE-Mioko eddy was centered at about (16°W, 26°N), with maximum SLA of 16 cm at the eddy center (Figure 3c).

From mid-October until 2 November 2008 (Figure 3d), the structure moved toward the east-southeast with a mean velocity of ~2 km d^{-1}. The core of the eddy approached the continental slope and the original near-circular shape of the structure took on an elongated shape. The SLA maximum values in the core of the eddy reached 20 cm, the SLA radial gradients increased accordingly and the geostrophic velocity reached a maximum value of 32 cm s^{-1}. On 2 November AE-Mioko started a new migration, now toward the northwest with twice the October velocity (~ 4 km d^{-1}), and in mid-November, it merged with another anticyclone (Figures 3e and 3f). As shown in Figures 1 and 3e, on 9–11 November AE-Mioko had an elongated shape with a southeast-northwest axis and maximum geostrophic velocities of about 34 cm s^{-1}; at this time, the eastern half of the eddy was sampled with the Nu-shuttle. During the ship sampling, the eddy was approximately centered at the same position as when initially detected in mid-October, but with clear evidence of deformation after having interacted with the surrounding structures (Figure 1).

The November eddy migration is confirmed by the temporal rate of change of SLA (hereinafter SLA tendency). *Flexas et al*. [2006] use a similar approach to investigate the displacement and deformation of an eddy in the Western Mediterranean. The SLA tendency is computed here as the difference between SLA maps for two dates (5 and 15 November 2008) divided by the lag time. Maximum and minimum values of SLA tendency are not collocated in the center of AE-Mioko but on the edges (Figure 4). This indicates that the eddy is not amplifying or decaying but propagating, see *Pascual et al*. [2004] and *Gomis et al*. [2005] for more details on this interpretation. In this case, the regions of negative/positive SLA tendency are found at the southeastern/northwestern part of AE-Mioko, respectively, which is consistent with a northwestward migration during the 10 day period, given it is an anticyclonic eddy. This journey is confirmed by an alternative method based on a new SSH-based eddy tracker (E. Mason et al., A new sea surface height based code for oceanic mesoscale eddy tracking, submitted to *Journal of Atmospheric and Oceanic Technology*, 2014). For the period between 29 October and 12 November, which includes the in situ sampling, the eddy tracker estimates a mean eddy's propagation velocity and direction of 4.1 km d^{-1} and 290.1°, respectively.

3.2. Horizontal and Vertical Structure

Figure 5 shows the spatial distribution of temperature, salinity and density at three depths (30, 65, and 100 m), as estimated after the OSI of the Nu-Shuttle observations. AE-Mioko has a slightly tilted warm core of 22.4°C. The salinity fields show a more heterogeneous spatial pattern: a dipole structure appears at 30 and 65 m depth with salinity values of 37.10 in the northern part and 36.9 in the southern part. However, at 100 m, the salinity field is more uniform than in the upper levels with a core of 37.0. The density maps, with values of about 25.7 kg m^{-3} at all three depths, are dominated by the temperature field. AE-Mioko is surrounded by denser waters (~26.0 kg m^{-3}) to the north, associated with the cyclonic eddy observed in the altimetry maps (Figure 1).

The near-surface (down to 130 m) hydrographic vertical structure of the eddy is summarized in Figure 6; the four transects crossing the eastern half of the eddy through its eastern edge (transect (i)) or its center (transect (iv)) (Figure 1). At the eastern end, transect (i) does not provide clear evidence of a dense core, showing instead a homogeneous horizontal layer in temperature and a very weak horizontal density

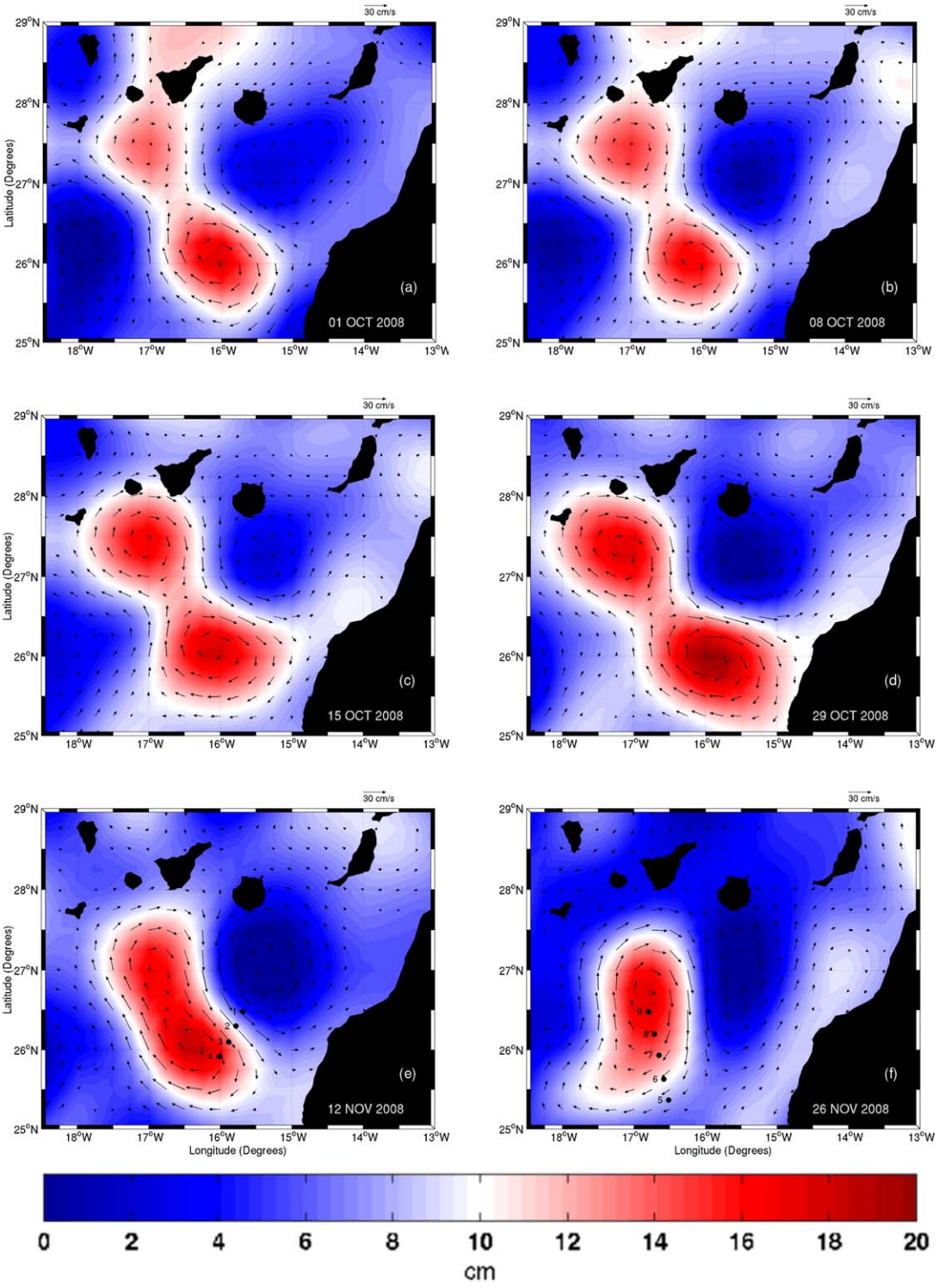

Figure 3. Maps of SLA (cm) and associated geostrophic velocity anomaly (cm s^{-1}). From left to right and top to bottom: 1, 8, 15, and 29 October and 12 and 26 November 2008. Black dots correspond to CTD casts performed on 12 and 28 November 2008.

gradient; this transect may be considered as representative of the hydrographic conditions outside of the eddy. Transect (ii) represents a transition zone where the horizontal temperature and density gradients increase, and the warm core of AE-Mioko becomes visible. Relatively low density values (25.8 kg m^{-3})

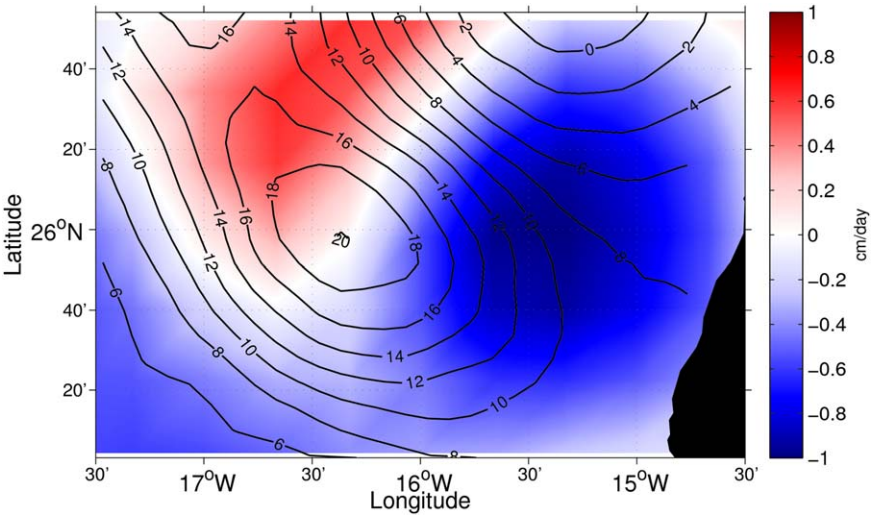

Figure 4. Difference between SLA maps (background color field) for 5 and 15 November 2008 divided by time lag (units are cm d^{-1}). The isolines correspond to SLA (cm) for 10 November 2008.

appear in transect (ii), but only reach down to ~75 m and are horizontally deformed (there are two troughs related to the temperature and salinity distributions at that depth, see Figure 5). Transects (iii) and (iv) are representative of the properties in the eddy center, where the 26.1 kg m^{-3} isopycnal reaches more than 120 m depth.

The CTD data, gathered shortly after the Nu-Shuttle sampling, confirm that AE-Mioko was a shallow eddy (Figure 7) extending no deeper than 250 m. The T/S diagram (not shown) using both CTD and Nu-shuttle data reveals that the top 250 m of the study area are dominated by North Atlantic Central Waters (NACW), with salinity values between 36.8 and 37.1 and temperatures between 21.5°C and 22.3°C.

3.3. Geostrophic and Ageostrophic Circulation

The dynamic height (DH) is calculated from the Nu-shuttle optimally interpolated density fields setting 130 m as the reference level. The DH and geostrophic velocity fields illustrate that the Nu-shuttle sampled the core and the southeastern portion of the eddy (Figure 5). At 30 m, the difference in DH between the eddy core and its edge is 13 cm, very similar to the differences calculated at the sea surface through altimetry. This result gives us confidence in the use of such a shallow reference level for the geostrophic calculations; comparison with the ADCP (see below) also justifies this choice.

At 30 m, the maximum DH gradients, and associated geostrophic velocities (~35 cm s^{-1}), are found at the northeast and southwest edges of AE-Mioko, between transects (ii) and (iii) (Figure 5). At 100 m, the DH gradient is significantly reduced and the geostrophic velocities are everywhere less than 5 cm s^{-1}. The outer end of the eddy is located between transects (i) and (ii), where the geostrophic velocity reverses direction. The existence of such a transition zone is also evidenced by hydrographic data, mainly temperature. Along transect (i) we can identify the edge of another independent structure, apparently located between AE-Mioko and the African coast. Unfortunately, no additional in situ data closer to the coast are available to investigate this interaction.

A comparison of the velocity fields in the uppermost layer (0–30 m), estimated either from the altimetry or OSI density fields, with the actual VM-ADCP velocity measurements and the drifter's trajectory also gives good agreement and grants further confidence in the 130 m reference level (Figure 8a). The geostrophic velocity derived from the Nu-shuttle hydrographic data and the VM-ADCP measurements are coherent, both showing the presence of the anticyclonic structure. Some differences in the direction are found, particularly at the eastern boundary of the domain. Regarding magnitude, the VM-ADCP produces slightly higher velocities, as expected. The relatively small differences between geostrophic and actual velocities may be related to the shallowness of the reference level, but may also indicate the presence of cyclostrophic acceleration. To assess the importance of any cyclostrophic acceleration, a simple scale analysis is

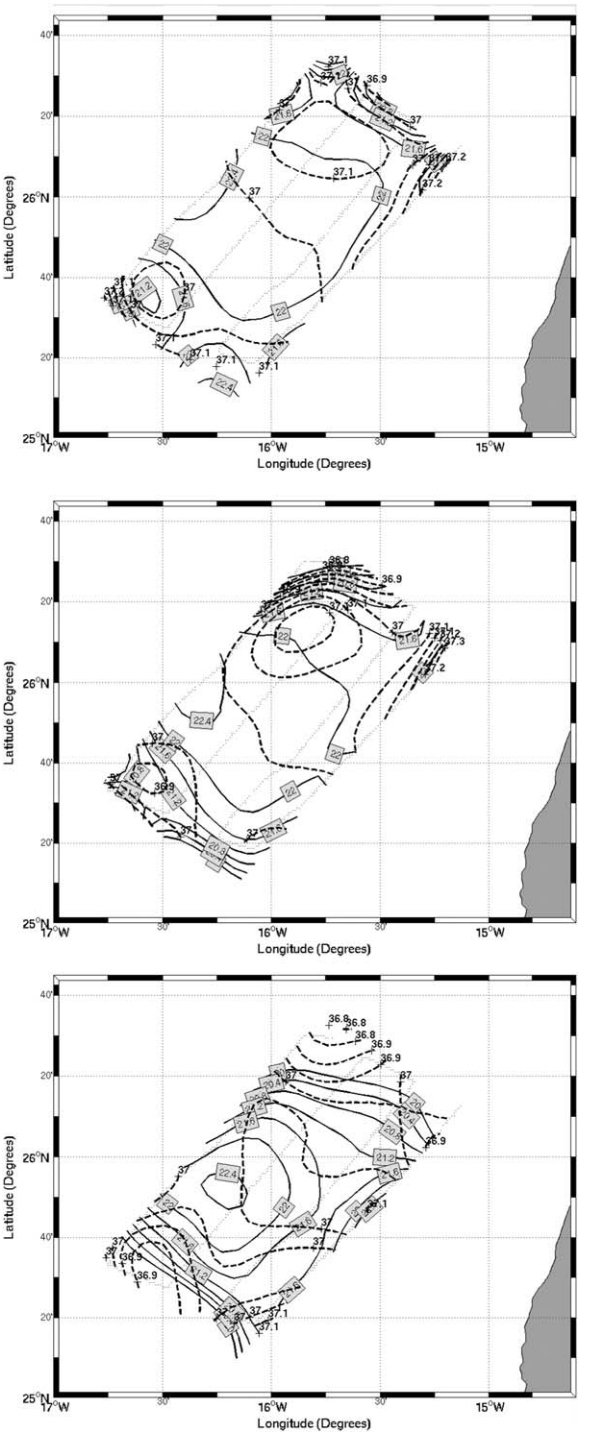

Figure 5. Interpolated maps of temperature in °C (solid line and labels inside squares) and salinity (dashed lines) at 30, 65, and 100 m (from top to bottom, respectively). Next page: (left) Interpolated density (kg m^{-3}); (right) dynamic height (cm) and associated geostrophic velocity (cm s^{-1}) at 30, 65, and 100 m (from top to bottom, respectively). The reference level (motionless) for the geostrophic velocity calculation is 130 m.

conducted by considering the ratio of cyclostrophic acceleration to the Coriolis acceleration. Using mean characteristic length and velocity values for the study area, this ratio is smaller than 0.1, suggesting that the cyclostrophic acceleration associated with the anticyclonic eddy is not dominant. Other authors have found super-geostrophic eddies (up to 20% difference between actual and geostrophic velocities) in very energetic areas such the Alboran Sea [*Gomis et al*., 2001].

To better characterize the transition zone between transects, the relative geostrophic vorticity has been computed. Figure 8b shows a horizontal field of relative vorticity at 65 m computed from the in situ data. Negative values are observed over most of the structure, reaching minima of about -4×10^{-5} s^{-1}; however, the vorticity changes to positive values ($\sim 2 \times 10^{-5}$ s^{-1}) along the southeastern boundary of the domain, specifically between transects (i) and (ii). These values are of the same order as the local planetary vorticity, which is about 6×10^{-5} s^{-1}.

Figure 8b also shows the vertical velocity field at 65 m computed using the Omega equation (equation (1)). Downward (negative) and upward (positive) velocities are diagnosed, respectively, in the northern and southern part of the eddy, of the order of 2 m d^{-1}. Additionally, a dipole of positive/negative values is found in the southwestern corner of the domain. The center of AE-Mioko is inactive, characterized by near-zero values of vertical motion.

3.4. Fusion of Two Anticyclones

Satellite altimetry images from 16 to 26 November (we show only 26 November, Figure 3f) reveal a fusion of AE-Mioko with another anticyclonic eddy located further northwest. We may examine the changes in the vertical structure of the eddy from the hydrographic data collected before and after the fusion. During

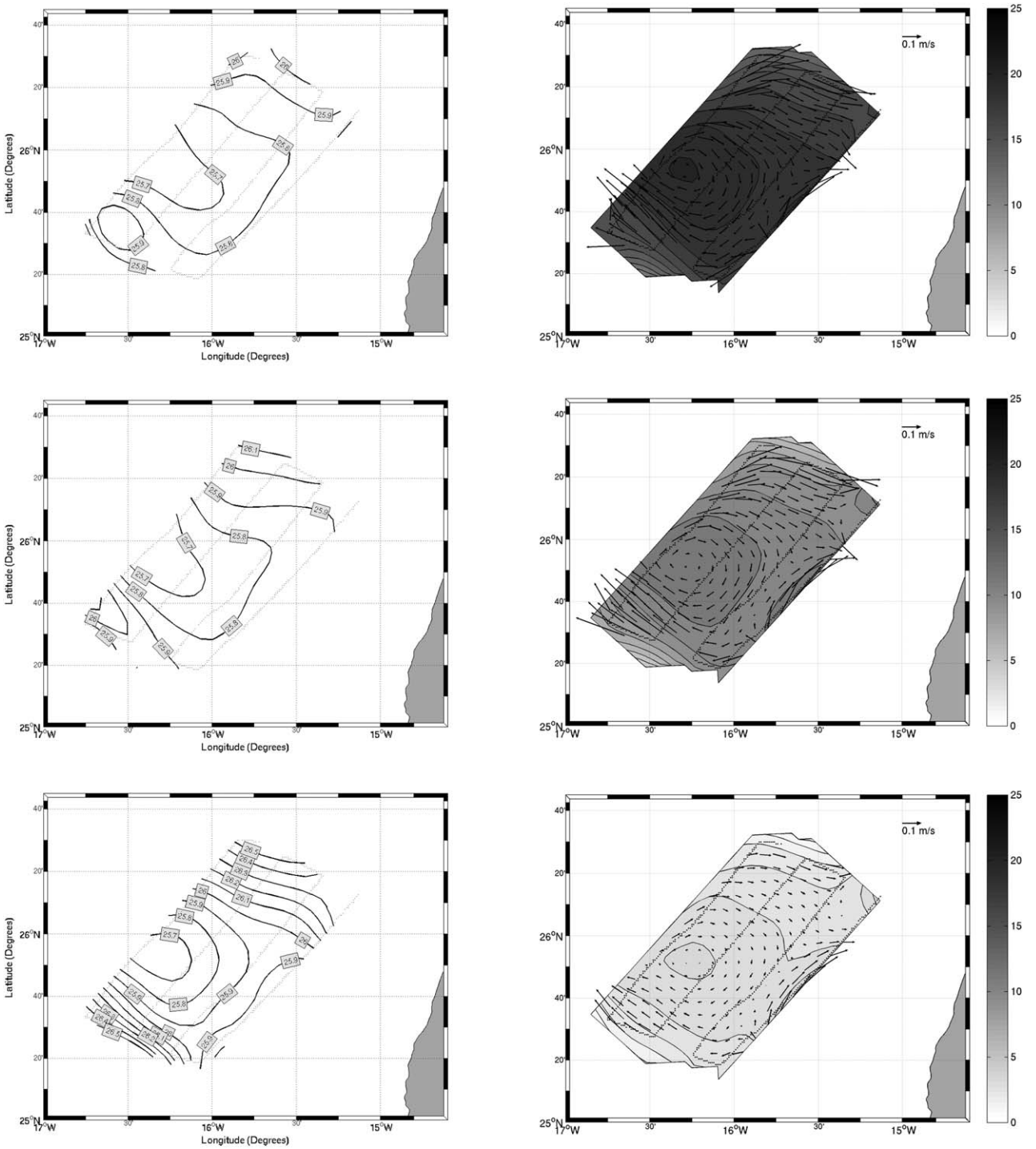

Figure 5. (continued)

the fusion, the eddy was conditioned by the presence of a relatively intense and small cyclone to the northeast (Figures 1 and 3), with CTD station 1 actually located inside this cyclone (Figure 3e). Therefore, in order to assess the temporal evolution of the vertical structure of the eddy interior, we ignore the horizontal temperature gradients between stations 1 and 2 (Figure 7a) and consider only those stations pertaining to the edge and interior of the anticyclonic eddy as clearly illustrated in Figures 3e and 3f, i.e., stations 2, 3, and 4 (before the fusion) and 6, 7, and 8 (after the fusion).

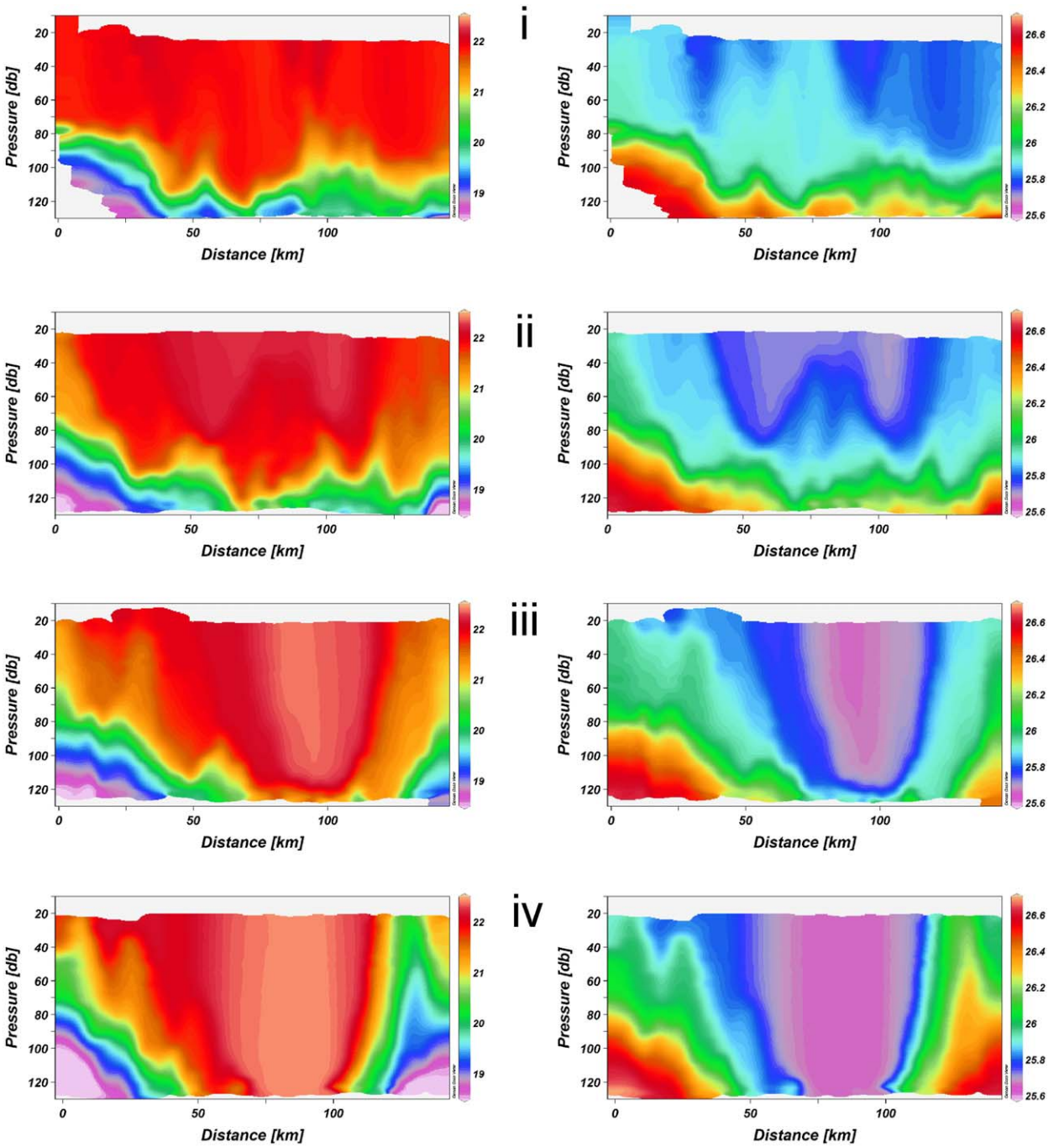

Figure 6. Vertical sections of temperature (°C) and density (kg m^{-3}) from Nu-shuttle data. From top to bottom: transects (i), (ii), (iii), and (iv).

The thermal structure of the eddy displays some substantial temporal changes (Figures 7a and 7b). A comparison between the eddy stations before and after the fusion reveals maximum differences in density of 0.3 kg m^{-3} around 100 m (not shown) and up to 1°C in temperature not only at 100 m, but also between 300 and 400 m depth (Figure 7b). To better determine the vertical extent of the eddy before and after the fusion, we may look at its depth structure in isothermal coordinates (Figures 7c and 7d). In this coordinate system, the depth of the isotherms, z, turns into the dependent variable and their slope is given by $\partial z/\partial x$. In order to assess whether the isotherms are or are not affected by the antiocyclonic eddy, we have defined a threshold slope of 0.4×10^{-3} between the eddy interior and its edge, i.e., vertical differences of at least

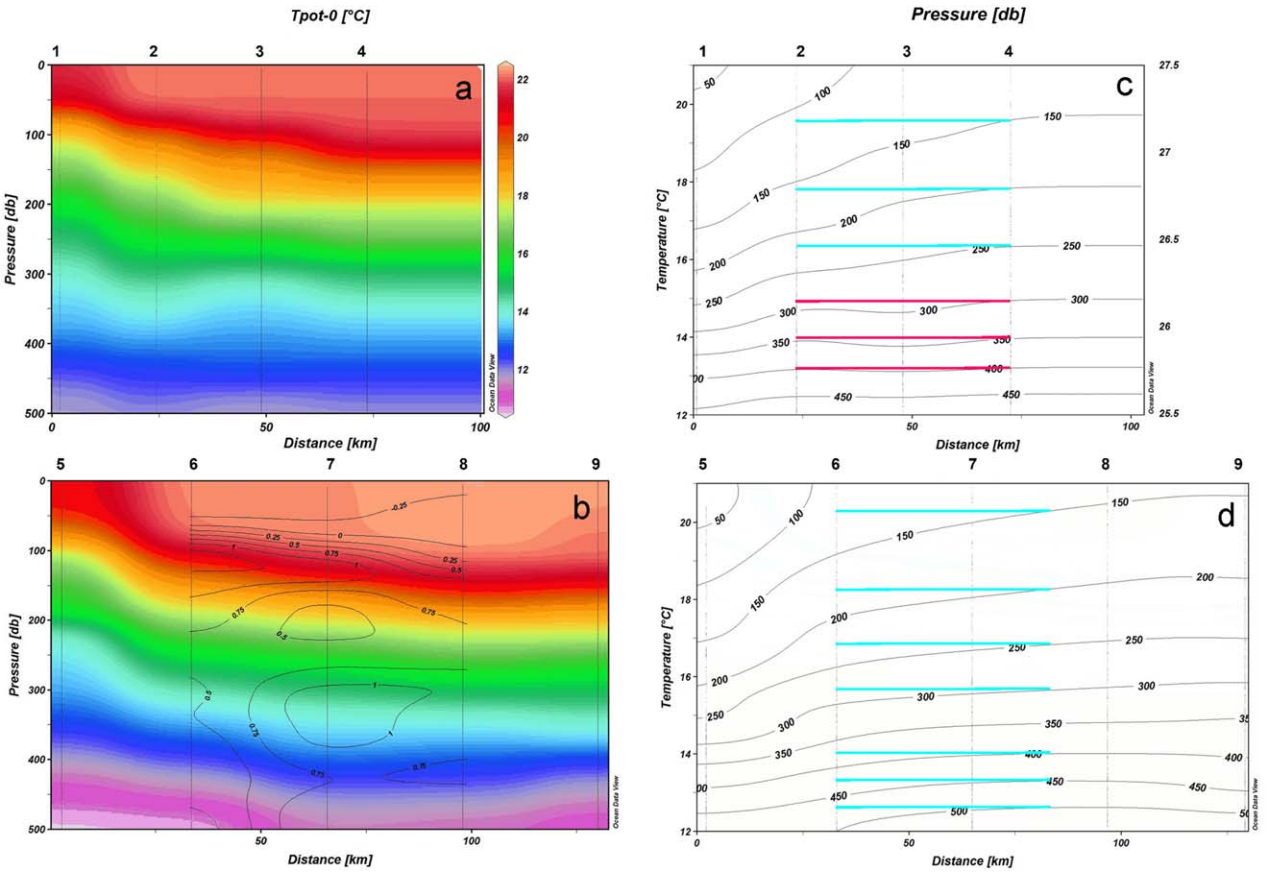

Figure 7. (a, b) Vertical sections of temperature (°C) as function of depth (db). (c, d) depth (db) as function of temperature (°C) as obtained from the ship CTD data: (top) stations 1–4 moving north to south, before the fusion, (bottom) stations 5–9 moving south to north, after the fusion. Black solid lines in Figure 7b represent the difference in temperature between pairs of stations from the edge to the interior of the eddy (st. 2–st.6; st.3–st.7; st. 4–st.8). Blue/red lines in the Figures 7c and 7d correspond to isolines that meet/not meet the slope criterion (slope higher than 0.4×10^{-3}).

20 m in 50 km horizontal distance; when the slope of an isotherm exceeds this value we will consider it to be part of the eddy. Based on this criterion, AE-Mioko was a relatively shallow feature before its fusion, reaching only down to about 250 m deep (Figure 7c). In contrast, after the fusion all isotherms represented in Figure 7d (down to at least 500 m) met the criterion to be considered as part of the eddy, clearly pointing to the presence of a much deeper structure. This result sustains the idea that the northwestern anticyclonic eddy was originally quite deep, generated through the barotropic interaction of the Canary Current with the islands, so that it dominated the fused eddy. A detailed numerical study of the merging process has been reported by *Rodríguez-Marroyo* [2011], who analyzes the factors controlling the fusion of two anticyclones under the influence of a cyclone.

4. Summary and Concluding Remarks

The eastern-boundary Canary Current system is the loci of numerous locally generated mesoscale structures, of either barotropic or baroclinic origin, which experience substantial interactions. This work has focused on the dynamics of AE-Mioko, a shallow mesoscale anticyclonic eddy. The horizontal and vertical structure of this eddy and its temporal displacement/deformation have been described using multiparametric sampling and remote sensing data, and the geostrophic and ageostrophic circulation have been diagnosed based on the geostrophic balance and the QG-Omega equation.

AE-Mioko was a warm-core shallow (∼250 m depth) anticyclonic eddy located south of the Canary Islands. This eddy moved within a relatively small region until it eventually merged with another eddy. Altimetry and in situ data clearly show that the eddy was not isolated, being surrounded by many other structures.

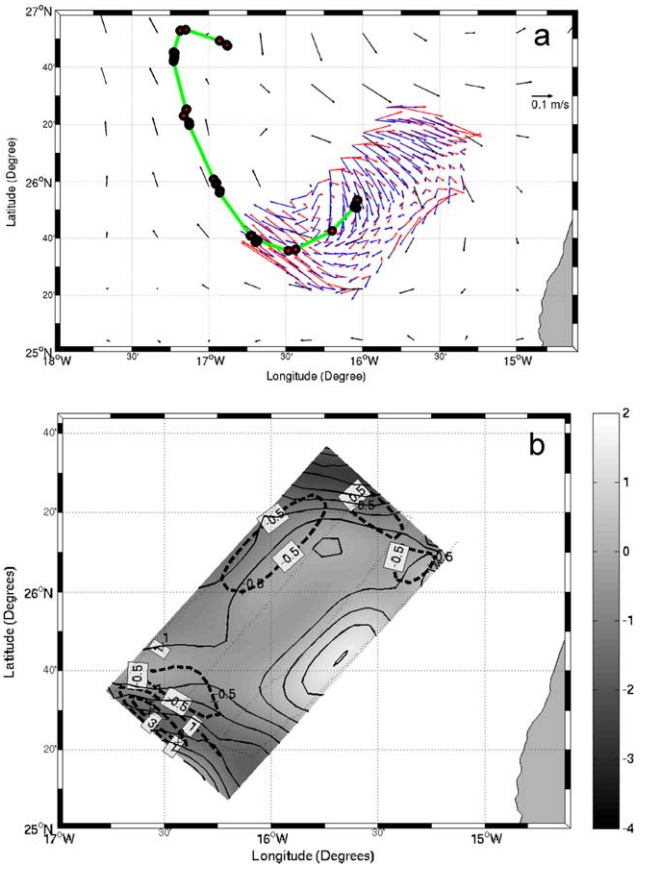

Figure 8. (a) Velocity (cm s^{-1}) vectors at 30 m as determined by the VM-ADCP 75KHz (blue), geostrophic approximation from hydrographic data (red) and altimetry (black). Green line corresponds to the drifter's trajectory from 12 to 20 November 2008 with tick marks indicating the daily positions. (b) Relative geostrophic vorticity (background color with solid line, units are 10^{-5} s^{-1}) and quasi-geostrophic vertical velocity (dashed line, units are m d^{-1}) at 65 m depth.

The interaction and long-distance migration of similar mesoscale structures has recently been studied by *Sangrà et al*. [2009]. These authors reported the existence of a Canary Eddy Corridor, where long-lived eddies (2 months or longer) such as AE-Mioko, originate south of the Canary Islands and propagate to the west, contributing to the export of organic matter from nutrient-rich areas near the African coast to the interior ocean. In our particular case, the motion of AE-Mioko was constrained by interactions with adjacent structures. Indeed, the in situ sampling occurred when the structure was beginning to merge with another anticyclonic eddy [*Rodríguez-Marroyo et al*., 2011]. This merging process was tracked by a subsurface drifter (drogued at about 100 m) deployed in the center of AE-Mioko (Figures 3 and 8a).

The distributions of the different properties within AE-Mioko confirm that, before the fusion, it was a shallow anticyclonic eddy. The density field was controlled by the temperature distribution, which was substantially altered only down to about 250 m (Figure 7). The geostrophic surface velocity is in good agreement with the surface geostrophic velocity inferred from altimetry measurements. Moreover, the horizontal velocity field, as measured by the VM-ADCP, coincides with the geostrophic velocity field calculated from the Nu-shuttle density field with a no-motion reference level at 130 m. The small differences observed (actual velocities are slightly higher than geostrophic) could be explained by the shallowness of the reference level. These results confirm that AE-Mioko was most likely generated at the coastal upwelling frontal zone.

The horizontal velocity field shows that AE-Mioko had relatively high surface velocities, with maximum values exceeding 30 cm s^{-1}; the relatively small differences between the observed and geostrophic velocities also confirm that AE-Mioko was in near-geostrophic balance. Maximum QG vertical velocities (± 2 m d^{-1}) are located along the northern and southern boundaries of the shallow eddy. Recently, *Benítez-Barrios et al*. [2011] also examined the horizontal and vertical transport associated with mesoscale eddies south of the Canary Islands and found that the vertical velocities reached substantially larger maximum values, up to $-18/+12$ m d^{-1}. In their case, they sampled a relatively deep anticyclonic eddy ($\sim$500 m), situated to the north of our study area.

There have been several observational and numerical studies that have contributed to improve our understanding of the mechanisms for eddy generation in the Canary region [*Piedeleu et al*., 2009; *Jiménez et al*., 2008; *Mason et al*., 2011, 2012]. These studies, based on the typical speed of the Canary Current and the overlying northeasterly winds, estimate that about 10 eddies are generated every year at Gran Canaria through either topographic or wind-shear effects. These eddies, however, are much deeper (500–1000 m) and significantly smaller (diameter 50 km) than the eddy reported here. Our results sustain the hypothesis

that many eddies such as AE-Mioko may be generated through a different mechanism, namely the baroclinic instability of the coastal upwelling jet. Such a mechanism would lead to relatively shallow (no deeper than the frontal upwelling system itself, or about 200–300 m) and large (radius >100 km) eddies [*Benítez-Barrios et al*., 2011]. A similar mechanism has been proposed in the California upwelling system to explain the high levels of mesoscale variability [*Marchesiello and Estrade*, 2009; *Marchesiello et al*., 2003].

The existence of other mesoscale structures is important for the posterior development of eddies in our study area. *Barton et al*. [1998] reported the presence of a quasi-permanent cyclonic eddy situated between Canary Islands and the African coast such as happened in autumn 2008, during the sampling of AE-Mioko. The interaction of this cyclonic eddy with AE-Mioko has been studied numerically by *Rodríguez-Marroyo et al*. [2011], confirming the static behavior of the cyclonic structure for nearly 2 months.

It is necessary to further improve our understanding of those mechanisms controlling the origin, propagation and interactions of mesoscale coastal structures. Mesoscale eddies such as AE-Mioko play a two-fold role in the fertilization of the upper interior ocean: (i) their lateral displacement leads to open/coastal water exchange, responsible for the redistribution of organic carbon and nutrients used by marine biota, and (ii) the associated vertical motions locally enhance nutrient concentrations in the upper layers, also favoring photosynthetic activity. In order to understand their dynamics, both field and numerical studies are necessary. Field experiments require synergetic approaches with the help of multiple sensors. Our study represents a step in this direction, despite sampling limitations in terms of limited spatial coverage, the lack of repeated measurements, and the low spatial resolution of the altimetry data. To better evaluate the vertical and horizontal exchanges it would be necessary to improve the sampling resolution in order to capture smaller structures (1–15 km) whose contribution has not been well-quantified so far, for instance, using a fleet of gliders in combination with CTDs sampling from a ship. These observational efforts shall go together with increased resolution circulation models, capable of resolving submesoscale processes.

Acknowledgments

This work has been done in the framework of the CANOA project (CTM2005-00444/MAR) funded by the Spanish Marine Science and Technology Program. We would like to thank all the crew and scientific staff on board R/V Sarmiento de Gamboa for their efficient collaboration during the cruise CANOA-08B. Figures 6 and 7 have been done using Ocean Data View [*Schlitzer*, 2008]. M. Emelianov contract was partially funded by contracts ESP2007-65667-C04-01 (MIDAS-5) and 2009SGR378. Simón Ruiz contract is funded by the Ramón y Cajal program of the Spanish Minister of Economy and Competitivity. E. Mason is supported by a Spanish government JAE-Doc grant (CSIC), cofinanced by FSE.

References

Allen, J. T., D. A. Smeed, J. Tintoré, and S. Ruiz (2001), Mesoscale subduction at the Almeria-Oran front: Part 1: Agesotrophic flow, *J. Mar. Syst*., *30*, 263–285.

Arístegui, J., P. Sangrà, S. Hernández-León, M. Cantón, A. Hernández-Guerra, and J. Kerling (1994), Island-induced eddies in the Canary Islands, *Deep Sea Res., Part I*, *41*, 1509–1525.

Arístegui, J., et al. (1997), The influence of island-generated eddies on chlorophyll distribution: A study of mesoscale variation around Gran Canaria, *Deep Sea Res., Part I*, *44*, 71–96, doi:10.1016/S0967-0637(96)00093-3.

Barton, E. D. (1998), Eastern boundary of the North Atlantic: Northwest Africa and Iberia: Coastal segment (18, E), in *The Sea*, vol. 11, edited by A. R. Robinson and K. H. Brink, pp. 633–657, John Wiley, New York.

Barton, E. D., et al. (1998), The transition zone of the Canary Current upwelling region, *Prog. Oceanogr*., *41*, 455–504.

Barton, E. D., G. Basterretxea, P. Flament, E. G. Mitchelson-Jacob, B. Jones, J. Arístegui, and H. Felix (2000), Lee region of Gran Canary, *J. Geophys. Res*., *105*, 17,173–17,193.

Barton, E. D., J. Arístegui, P. Tett, and E. Navarro-Pérez (2004), Variability in the Canary Islands area of filament-eddy exchanges, *Prog. Oceanogr*., *62*, 71–94.

Basterretxea, G., and J. Arístegui (2000), Mesoscale variability in phytoplankton biomass distribution and photosynthetic parameters in the Canary-NW African coastal transition zone, *Mar. Ecol. Prog. Ser*., *197*, 27–40.

Benítez-Barrios, V. M., J. L. Pelegrí, A. Hernández-Guerra, K. M. M. Lwiza, D. Gomis, P. Vélez-Belchí, and S. Hernández-León (2011), Three-dimensional circulation in the NW Africa coastal transition zone, *Prog. Oceanogr*., *91*, 516–533.

Borges, R., A. Hernández-Guerra, and L. Nykjaer (2004), Analysis of sea surface temperature time series of the south-eastern North Atlantic, *Int. J. Remote Sens*., *25*, 869–891.

Brachet, S., P.-Y. Le Traon, and C. Le Provost (2004), Mesoscale variability from a high-resolution model and from altimeter data in the North Atlantic Ocean, *J. Geophys. Res*., *109*, C12025, doi:10.1029/2004JC002360.

Brochier, T., E. Mason, M. Moyano, A. Berraho, F. Colas, P. Sangrà, S. Hernández-León, O. Ettahiri, and C. Lett (2011), Ichthyoplankton transport from the African coast to the Canary Islands, *J. Mar. Syst*., *87*, 109–122.

Emelianov, M., S. Ruiz, A. Pascual, and J. L. Pelegrí (2009), Observations of the evolution of a shallow baroclinic anticyclonic eddy off cape bojador, CANOA-08 cruise, R/V Sarmiento de Gamboa, internal report, 25 pp., Inst.de Cienc. del Mar, CSIC, Barcelona, Spain.

Flexas, M. M., D. Gomis, S. Ruiz, A. Pascual, and P. León (2006), In situ and satellite observations of the eastward migration of the Western Alborán Basin Gyre, *Prog. Oceanogr*., *70*(2–4), 486–509.

García-Muñoz, M., J. Arístegui, J. L. Pelegrí, A. Antoranz, A. Ojeda, and M. Torres (2005), Exchange of carbon by an upwelling filament off Cape Ghir (NW Africa), *J. Mar. Syst*., *54*(1–4), 83–95, doi:10.1016/j.jmarsys.2004.07.005.

Gomis, D., S. Ruiz, and M. A. Pedder (2001), Diagnostic analysis of the 3D ageostrophic circulation from a multivariate spatial interpolation of CTD and ADCP data, *Deep Sea Res., Part I*, *48*, 269–295.

Gomis, D., A. Pascual, and M. A. Pedder (2005), Errors in dynamical fields inferred from synoptic oceanographic cruise data: Part II: The impact of the lack of synopticity, *J. Mar. Syst*., *56*(3–4), 334–351.

González-Dávila, M., J. M. Santana-Casiano, D. De Armas, J. Escánez, and M. Suarez-Tangil (2006), The influence of island generated eddies on the carbon dioxide system, south of the Canary Islands, *Mar. Chem*., *99*(1–4), 177–190.

Griffiths, G. (1994), Using 3DF GPS heading for improving underway ADCP data, *J. Atmos. Oceanic Technol*., *11*(4), 1135–1143.

Hernández-Guerra, A., and L. Nykjaer (1997), Sea surface temperature variability off northwest Africa: 1981–1989, *Int. J. Remote Sens.*, *18*, 2539–2558.
Hernández-Guerra, A., J. Arístegui, M. Cantón, and L. Nykjaer (1993), Phytoplankton pigments patterns in the Canary Islands as determined using coastal zone colour scanner data, *Int. J. Remote Sens.*, *14*, 1431–1437.
Hoskins, B. J., I. Draghici, and H. C. Davies (1978), A new look at the omega-equation, *Q. J. R. Meteorol. Soc.*, *104*, 31–38.
Jiménez, B., P. Sangrà, and E. Mason (2008), A numerical study of the relative importance of wind and topographic forcing on oceanic eddies shedding by deep water islands, *Ocean Modell.*, *22*, 146–157.
Le Traon, P.-Y., F. Nadal, and N. Ducet (1998), An improved mapping method of multisatellite altimeter data, *J. Atmos. Oceanic Technol.*, *15*, 522–534.
Le Traon, P.-Y., Y. Faugère, F. Hernandez, J. Dorandeu, F. Mertz, and M. Ablain (2003), Can we merge GEOSAT Follow-On with TOPEX/POSEIDON and ERS-2 for an improved description of the ocean circulation?, *J. Atmos. Oceanic Technol.*, *20*, 889–895.
Marchesiello, P., and P. Estrade (2009), Eddy activity and mixing in upwelling systems: A comparative study of Northwest Africa and California regions, *Int. J. Earth Sci.*, *98*(2), 299–308.
Marchesiello, P., J. C. McWilliams, and A. F. Shchepetkin (2003), Equilibrium structure and dynamics of the California Current System, *J. Phys. Oceanogr.*, *33*, 753–783.
Mason, E., F. Colas, J. Molemaker, A. F. Shchepetkin, C. Troupin, J. C. McWilliams, and P. Sangrà (2011), Seasonal variability of the Canary Current: A numerical study, *J. Geophys. Res.*, *116*, C06001, doi:10.1029/2010JC006665.
Mason, E., F. Colas, and J. L. Pelegrí (2012), A Lagrangian study tracing water parcel origins in the Canary upwelling system, *Sci. Mar.*, *76*(S1), 79–94.
Pacheco, M., and A. Hernández-Guerra (1999), Seasonal variability of recurrent phytoplankton pigment patterns in the Canary Islands area, *Int. J. Remote Sens.*, *29*, 1405–1418.
Pascual A., D. Gomis, R. L. Haney, S. Ruiz (2004), A quasigeostrophic analysis of a meander in the Palamós Canyon: vertical velocity, geopotencial tendency and a relocation technique. *J. Phys. Oceanogr.*, *34*, 2274–2287.
Pascual, A., Y. Faugère, G. Larnicol, and P.-Y. Le Traon (2006), Improved description of the ocean mesoscale variability by combining four satellite altimeters, *Geophys. Res. Lett.*, *33*, L02611, doi:10.1029/2005GL024633.
Pascual, A., C. Boone, G. Larnicol, and P.-Y. Le Traon (2009), On the quality of real-time altimeter gridded fields: Comparison with in-situ data, *J. Atmos. Oceanic Technol.*, *26*, 556–569.
Pastor, M. V., J. Peña-Izquierdo, J. L. Pelegrí, and A. Marrero-Díaz (2012), Meridional changes in water properties off NW during November 2007/2008, *Cienc. Mar.*, *38*, 223–244.
Pelegrí, J. L., J. Arístegui, L. Cana, M. González-Dávila, A. Hernández-Guerra, S. Hernández-León, M. Montero, P. Sangrà, and M. Santana-Casiano (2005), Coupling between the open ocean and the coastal upwelling region off northwest Africa: Water recirculation and offshore pumping of organic matter, *J. Mar. Syst.*, *54*, 3–37.
Pelegrí, J. L., A. Marrero-Díaz, and A. W. Ratsimandresy (2006), Nutrient irrigation of the North Atlantic, *Prog. Oceanogr.*, *70*, 366–406.
Peña-Izquierdo, J., J. L. Pelegrí, M. V. Pastor, P. Castellanos, M. Emelianov, M. Gasser, J. Salvador, and E. Vázquez-Domínguez (2012), The continental slope current system between Cape Verde and the Canary Islands, *Sci. Mar.*, *76*(S1), 65–78.
Piedeleu, M., P. Sangrà, A. Sánchez-Vidal, J. Fabrés, C. Gordo, and A. Calafat (2009), An observational study of oceanic eddy generation mechanisms by tall deep-water islands (Gran Canaria), *Geophys. Res. Lett.*, *36*, L14605, doi:10.1029/2008GL037010.
Pinot, J. M., J. Tintore, and D. P. Wang (1996), A study of the omega equation for diagnosing vertical motions at ocean fronts, *J. Mar. Res.*, *54*, 239–259.
Rio, M.-H., and F. Hernandez (2004), A mean dynamic topography computed over the world ocean from altimetry, in situ measurements and a geoid model, *J. Geophys. Res.*, *109*(C12), C12032, doi:10.1029/2003JC002226.
Rodriguez-Marroyo, R., A. Viúdez, and S. Ruiz (2011), Vortex merging in oceanic tripoles, *J. Phys. Oceanogr.*, *41*, 1239–1251.
Ruiz, S., J. Font, G. Griffiths, and A. Castellón (2002), Estimation of heading gyrocompass error using a GPS 3DF system: Impact on ADCP measurements, *Sci. Mar.*, *66*, 347–354.
Sangrà, P., J. L. Pelegrí, A. Hernández-Guerra, I. Arregui, J. M. Martín, A. Marrero-Díaz, A. Martínez, A. W. Ratsimandresy, and A. Rodríguez-Santana (2005), Life history of an anticyclonic eddy, *J. Geophys. Res.*, *110*, C03021, doi:10.1029/2004JC002526.
Sangrà, P., M. Auladell, A. Marrero-Díaz, J. L. Pelegrí, E. Fraile-Nuez, A. Rodríguez-Santana, J. M. Martín, E. Mason, and A. Hernández-Guerra (2007), On the nature of oceanic eddies shed by the island of Gran Canaria, *Deep Sea Res., Part I*, *54*, 687–709.
Sangrà, P., et al. (2009), The Canary Eddy Corridor: A major pathway for long-lived eddies in the subtropical North Atlantic, *Deep Sea Res., Part I, 56*, 2100–2114.
Schlitzer, R. (2008), *Ocean Data View*, Alfred Wegener Institute for Polar and Marine Research, Germany. [Available at http://odv.awi.de.]
SSALTO/DUACS User Handbook (2013), *(M)*SLA *and (M)*ADT Near-Real Time and Delayed Time Products, reference CLS-DOS-NT-06-034, CNES, Toulouse, France.
Thiébaux, H. J., and M. A. Pedder (1987), *Spatial Objective Analysis With Applications in Atmospheric Sciences*, 299 pp., Academic, New York.